The NINE: A Sabbatical Serving of Doubles

Glenn M. Thurman

Cuyamaca College, El Cajon, California

Abstract: Measures for nine doubles are presented. CCD images were obtained using an LX-200 16-inch telescope. MPO Canopus was used for reduction and calculation of separation and position angle. There is good agreement with historical data from the WDS, extrapolated to the epoch of observation.

Introduction

A double star is a pair of stars appearing close together in the sky. In general, the two stars move with respect to one another due to differences in proper motion. The proper motions are different because the two stars have different speeds and directions through space.

The apparent motion of stars through the sky is often straight line, or rectilinear, motion. If two stars in a double are gravitationally bound, orbiting a common center of mass, then each star's proper motion changes with time, and is not rectilinear. In this case each component of the double moves in an apparent ellipse with respect to the other star, as seen in the sky, and moves in a true ellipse about a common center of mass, in space. Evidence of orbital motion may be present in plots of historical measures.

Nine double stars were measured by the author during 2017, and the results are presented here. Much of the data reduction and analysis took place during my 2018 sabbatical and became part of my sabbatical report. Plots of secondary motion with respect to the primary, in cartesian coordinates, are presented.

Selection of the Pairs

Nine doubles were chosen from the Washington Double Star Catalog (WDS), Mason (2017). They were selected for the most favorable combination of air mass, separation, magnitude, likelihood the separation and position angle would have changed since the last historical observation, and pointing convenience.

Given in Table 1 are the WDS identifiers of the nine double stars observed. Also presented are the WDS Discoverer Designation; other names or identifiers, obtained from sky-map.org; and the WDS coordinates.

Observations and Reduction

The observations were made using a Meade LX200 16-inch f/10 reflecting telescope located at Gregory T. Thurman Memorial Observatory, in the foothills of East County San Diego, California, situated at about 2600 feet, under moderately dark skies.

Gregory T. Thurman Memorial Observatory. Greg made it all possible.

Greg

The CCD imaging was done using an SBIG STF-8300M monochrome camera, with a KAF-8300 CCD and 1.4-micron square pixels. Images were taken through a Johnson-Cousins Infra-Red filter (IC of the Johnson-Cousins UBVRI system). All images were flat-fielded and dark subtracted. The double star astrometry utility of the MPO Canopus software was used for the measures of separation and position angle.

Received May 27, 2020

	WDS Identifier	Discoverer Designation	Other Names/Identifiers	WDS Coordinates
1	1 01588+0908	CHE 30	TYC-623-1250-1	01:58:43.09 +09:07:50.3
2	2 03002-1110	BRT2627	TYC 5290-469-1	03:00:09.82 -11:10:25.3
3	3 04528-2521	B 75BC	USNOA2 0600-02025114	04:52:44.55 -25:21:18.4
4	4 04530-2758	BRT2858	USNOA2 0600-02027303	04:52:59.24 -27:58:21.3
5	5 06171-2243	HJ 3845	HD 43745	06:17:03.60 -22:42:54.8
6	6 06377+6129	BUP 91AC	8 LYN	06:37:41.38 +61:28:52.4
7	7 06389-2846	HJ 2334	TYC 5520-514-1	06:38:54.10 -28:46:42.6
8	8 07317-2356	ARA2056	USNOA2 0600-06512549	07:31:42.70 -23:55:33.6
9	9 07328-2332	ARA2058	USNOA2 0600-06586813	07:32:47.19 -23:31:51.3

Table 1: WDS Identifier, including Other Names/Identifiers, for the Primary Star of Each Double.

MPO Canopus "…provides a unique tool that directly computes the separation and position angle of any selected pair of stars (including the required precession calculation…)" Buchheim (2008). A few clicks of the mouse is all it takes.

Measurements

Table 2 lists the measures for the nine pairs observed, each measure being the average of some number of independent observations (separation or position angle). Also listed in the table is the number of observations obtained for each double, the Besselian Epoch, and the Standard Error of the Mean (SEM) for the measures that were averaged (separation or position angle).

Equation 1 was used to calculate the standard error of the mean (SEM) for the averaged observations (separation or position angle).

Equation 1: $$SEM = \frac{\sigma}{\sqrt{N}}$$

where is the number of observations averaged to give a particular measure of separation or position angle, and σ is the standard deviation (SD) of the observations.

Historical Data

Historical measures (WDS catalog) of separation and position angle for the pairs measured in this work were provided by Brian Mason. The historical measures of separation and position angle were combined with the measures of same in this work and plotted against time, in Appendix 1. These plots are one way to judge if my measures are reasonable compared to the historical data, and continue the trend.

The equation for a linear least squares fit to the data for each double appears on each graph. The equation can be used as an ephemeris for predicting separation or position angle for some time in the future.

Presented in Appendix 2 are Cartesian plots of the motion of the secondary star with respect to the primary, using the combined data, present and historical. The primary's position in each plot is represented by a cross. For each Cartesian plot, the x and y coordinates are given by Equations 2 and 3:

Equation 2: $x = \varrho \cos PA$

Equation 3: $y = \varrho \sin PA$

where ϱ (rho) equals the separation in arc seconds and PA equals the position angle in degrees.

The Appendix 2 plots of the motion of the secondary are also a way to judge the reasonableness of my data, and it is interesting to see if any orbital motion is apparent.

In the discussion below, all referred-to plots of rho vs. epoch or PA vs. epoch are presented in Appendix 1. All referred-to plots of motion of the secondary star are found in Appendix 2.

For the relatively short times covered by the historical data, most of the graphs in Appendices 1 and 2 appear linear, but might not be if the data spanned enough time. For the pair discussed immediately below, the graphs are NOT linear.

For **WDS 06171-2243**, before epoch 2000, the historical data for PA decreases with time to almost zero, then discontinuously (PA is passing through zero) jumps to about 359 degrees at epoch 2000 and continues to decrease. This would make for a hard to interpret, discontinuous graph. For the sake of a more read-

	WDS Catalog	Discovery Designation	Number of Observations	Besselian Epoch	Separation Arcseconds	SEM	Position Angle Degrees	SEM
1	01588+0908	CHE 30	6	2017.826	33.58	0.014	217.16	0.020
2	03002-1110	BRT2627	6	2017.811	12.07	0.014	247.22	0.037
3	04528-2521	B 75BC	5	2017.997	70.11	0.021	258.36	0.019
4	04530-2758	BRT2858	6	2017.901	7.89	0.087	223.91	0.056
5	06171-2243	HJ 3845	7	2017.904	62.23	0.034	357.99	0.015
6	06377+6129	BUP 91AC	11	2017.195	397.50	0.029	91.40	0.0045
7	06389-2846	HJ 2334	10	2017.951	11.29	0.016	120.57	0.080
8	07317-2356	ARA2056	5	2017.901	13.51	0.013	335.49	0.021
9	07328-2332	ARA2058	6	2017.899	20.66	0.0090	192.09	0.019

Table 2: Measures of Separation and Position Angle for the NINE Pairs.

able graph in Fig. 5b, 360 degrees were added to all PA's earlier than epoch 2000.

Continuing with WDS 06171-2243, there is curvature in the data of Figs. 5a and 5b, but no orbital motion is apparent in Fig. 5. At early epochs, the time rate of change of theta was large and negative, but smaller and negative, now. The rate of change is decreasing (as an absolute value), but is asymptotically approaching zero. At early epochs, the time rate of change of rho was small and positive, but larger now. The rate of change is increasing, but is asymptotically approaching a constant value. This behavior is expected by simple inspection of Fig. 5, and assuming only rectilinear motion. From inspection of the cartesian plots of secondary position for the other pairs, we would not expect large changes in the time rate of change of rho and theta.

Conclusion

Measures of separation and position angle were obtained and presented for nine double stars, using a 16-inch reflector for observations, and MPO Canopus for reduction. Plots of separation vs. Besselian epoch, and position angle vs. Besselian epoch, for the combined historical data and new measures, were presented here. Also presented here were graphs of motion of the secondary star, in Cartesian coordinates.

Acknowledgements

Thanks to Mathew James for helpful email discussions.

Thanks also to Brian Mason for cheerfully answering my questions, and for prompt delivery of requested WDS historical data.

MPO Canopus was used for the data reduction part of this work.

References

1) Buchheim, R.K., "CCD Measurements of Visual Double Stars," The Society for Astronomical Sciences 27th Annual Symposium on Telescope Science. Held May 20-22, 2008 at Big Bear Lake, CA. Published by the Society for Astronomical Sciences., p.13.

2) James, M. et al., 2019 "Measures of Ten Sco Doubles and the Determination of Two Orbits," JDSO: 15(3), 489 – 503.

3) Mason, B., "The Washington Double Star Catalog", 2017, Astrometry Department, U.S. Naval Observtory.

Glenn Thurman holds a Ph.D. in Chemistry (computational) from the University of California San Diego, and an M.S. in Astronomy from San Diego State University. He teaches Astronomy, Physics and Chemistry at Cuyamaca College, in the San Diego area.

Appendix 1: Plots of Separation / Position Angle vs. Besselian Epoch

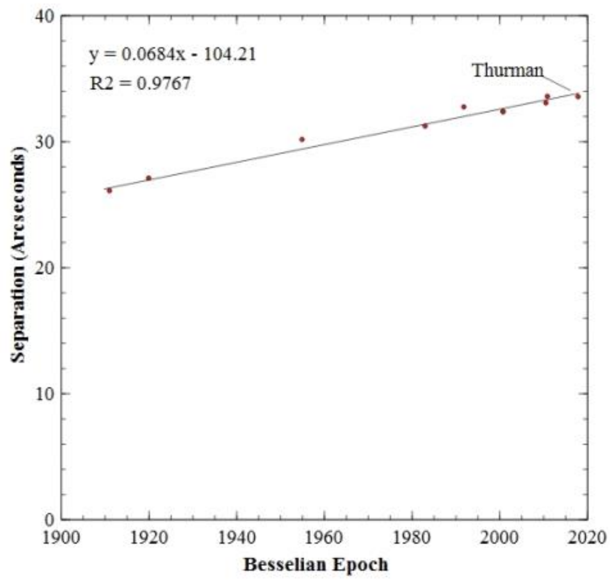

Figure 1a: WDS 01588+0908 Separation vs. Besselian Epoch.

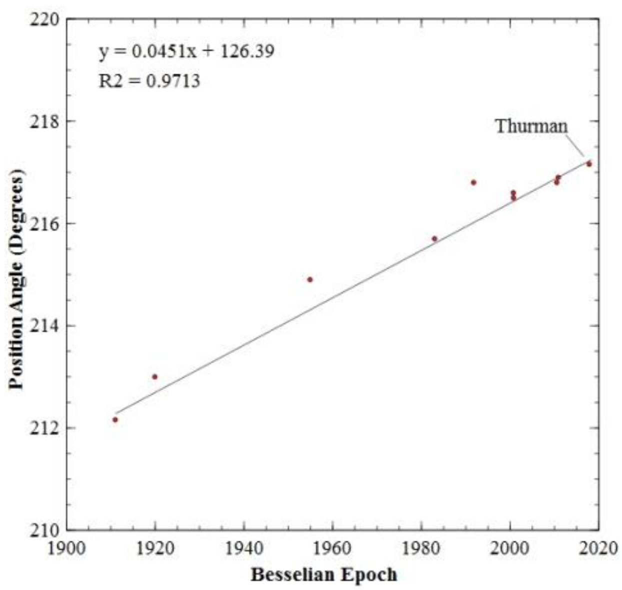

Figure 1b. WDS 01588+0908 Position Angle vs. Besselian Epoch.

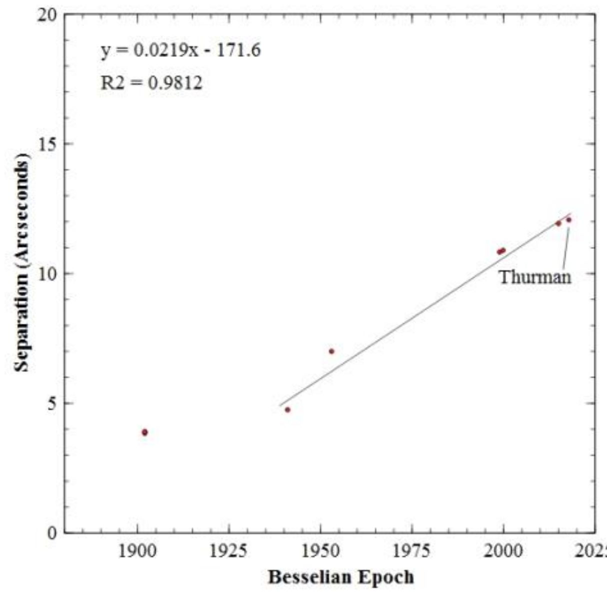

Figure 2a. WDS 03002-1110 Separation vs. Besselian Epoch.

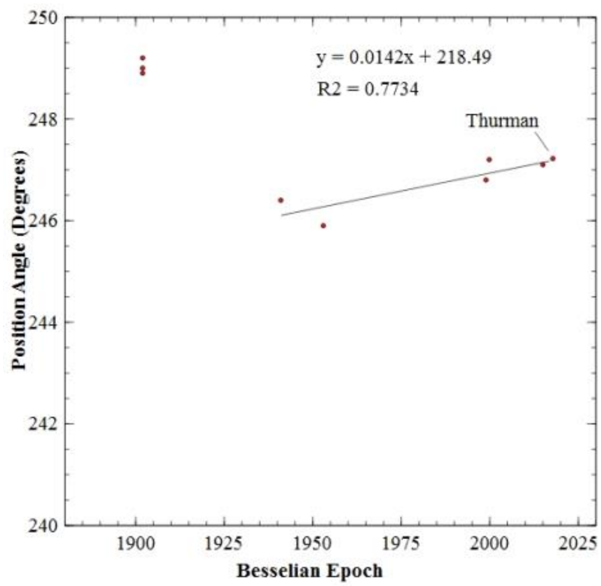

Figure 2b. WDS 03002-1110 Position Angle vs. Besselian Epoch.

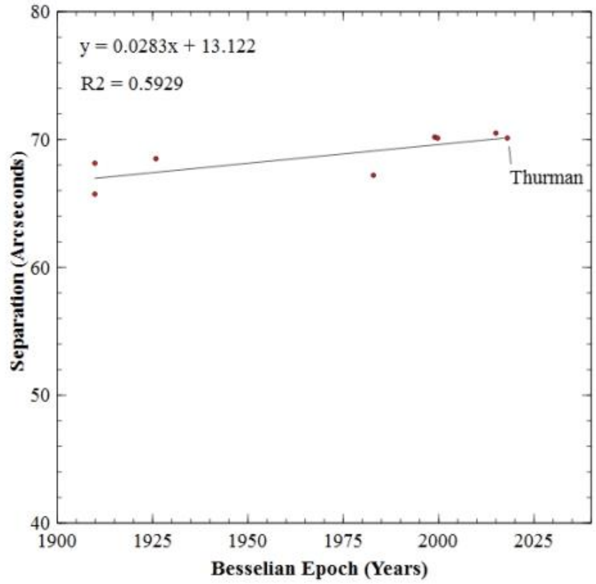

Figure 3a. WDS 04528-2521B Separation vs. Besselian Epoch.

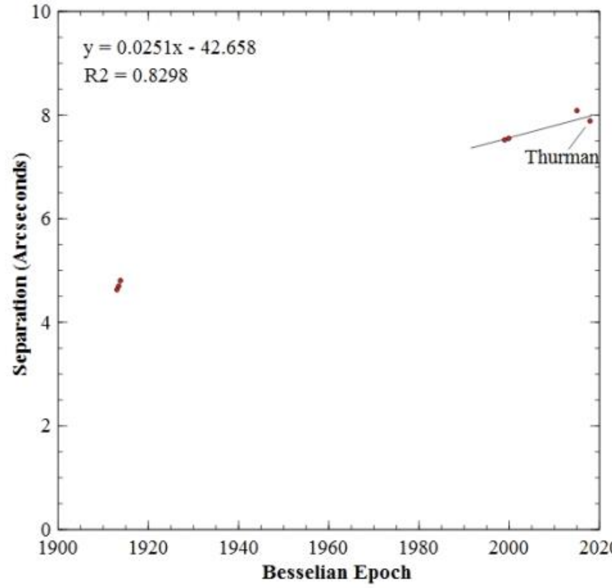

Figure 4a. WDS 04530-2758 Separation vs. Besselian Epoch.

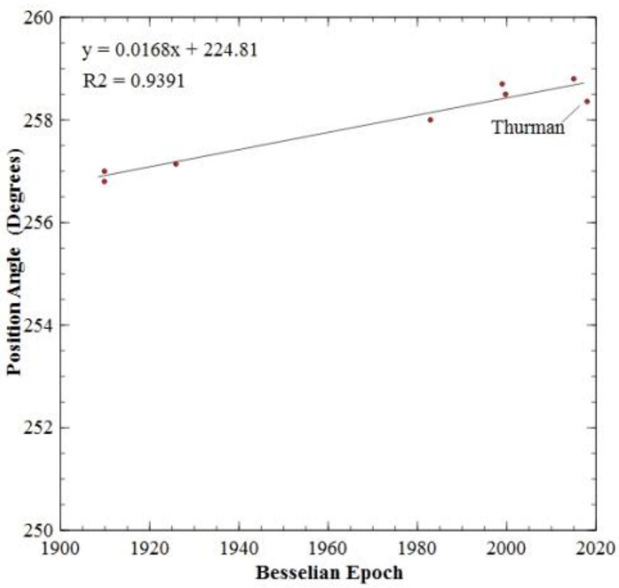

Figure 3b. WDS 04528-2521B Postion Angle vs. Besselian Epoch.

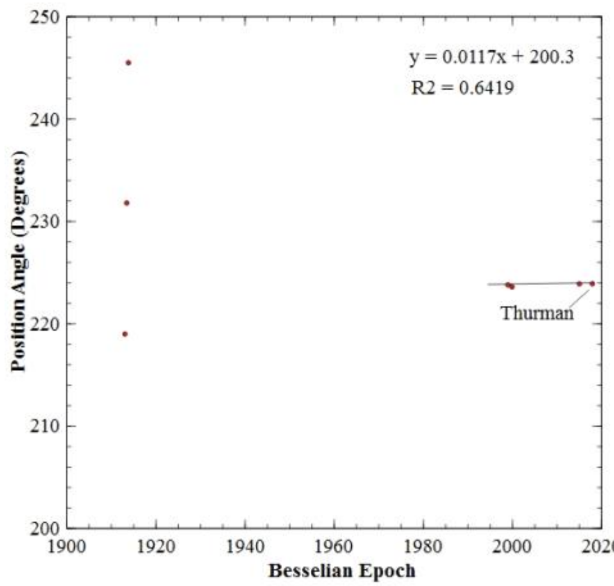

Figure 4b. WDS 04530-2758 Position Angle vs. Besselian Epoch.

The NINE: A Sabbatical Serving of Doubles

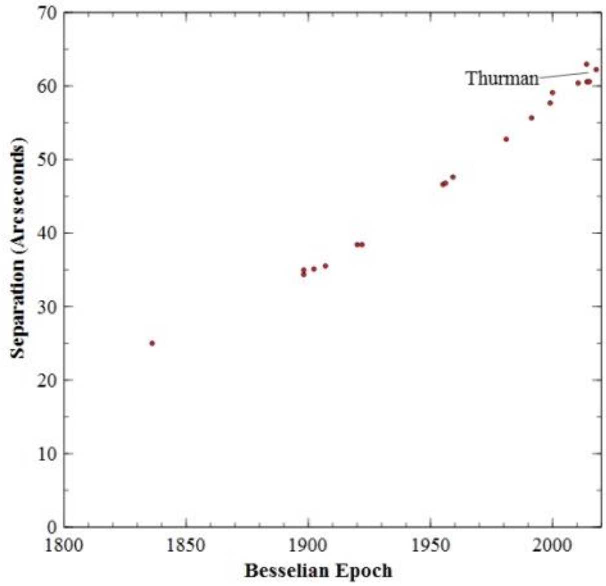

Figure 5a. WDS 06171-2243 Separation vs. Besselian Epoch.

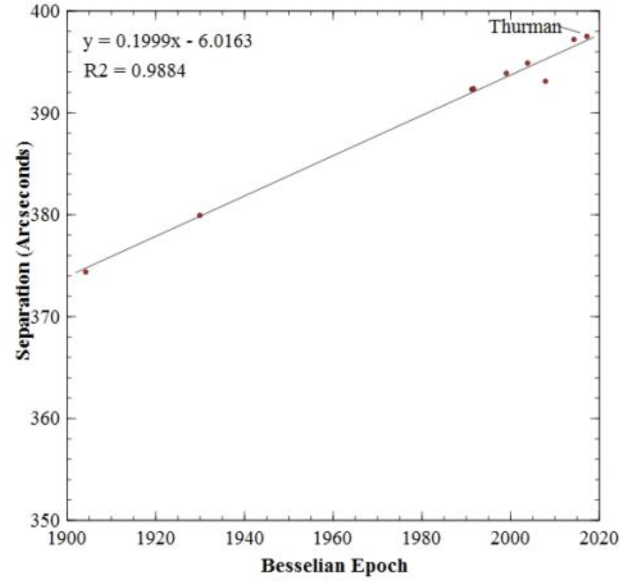

Figure 6a. WDS 06377+6129 Separation vs. Besselian Epoch.

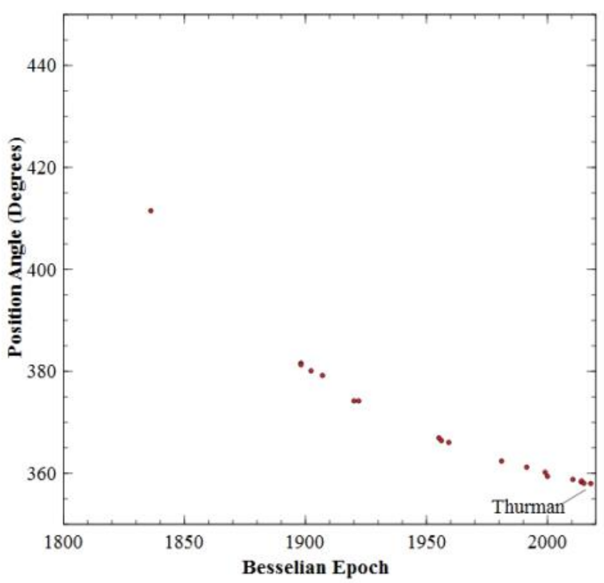

Figure 5b. WDS 06171-2243 Position Angle vs. Besselian Epoch.

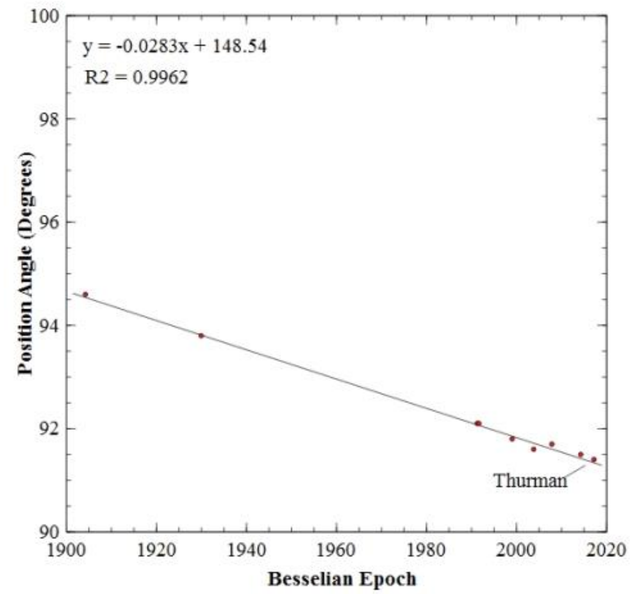

Figure 6b. WDS 06377+6129 Position Angle vs. Besselian Epoch.

The NINE: A Sabbatical Serving of Doubles

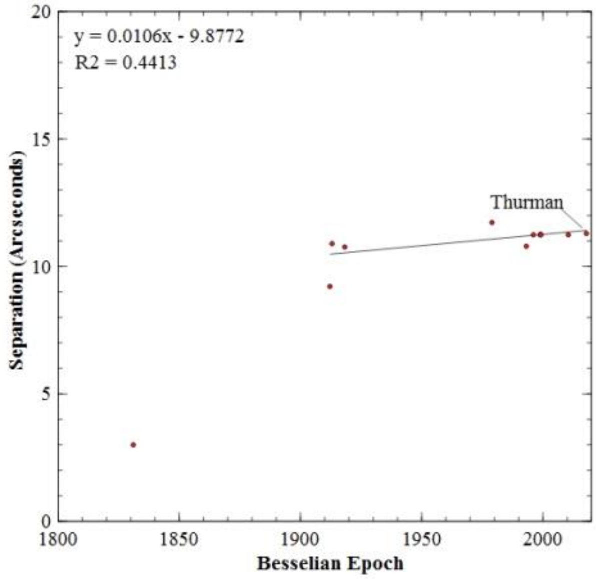

Figure 7a. WDS 06389-2846 Separation vs. Besselian Epoch.

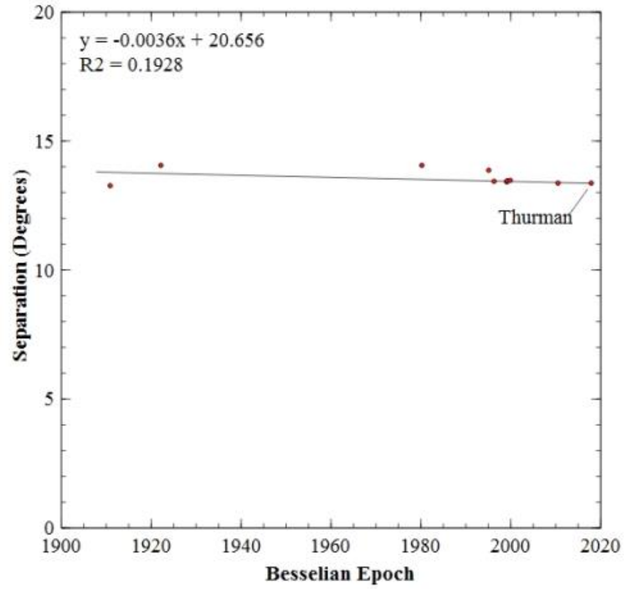

Figure 8a. WDS 07317-2356 Separation vs. Besselian Epoch.

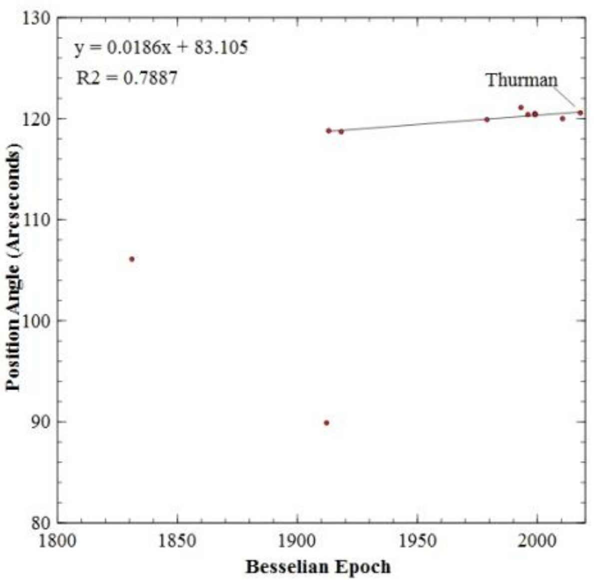

Figure 7b. WDS 06389-2846 Position Angle vs. Besselian Epoch.

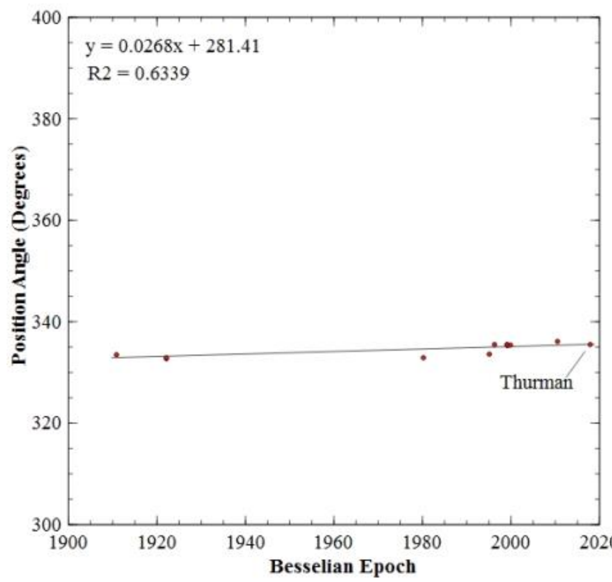

Figure 8b. WDS 07317-2356 Position Angle vs. Besselian Epoch.

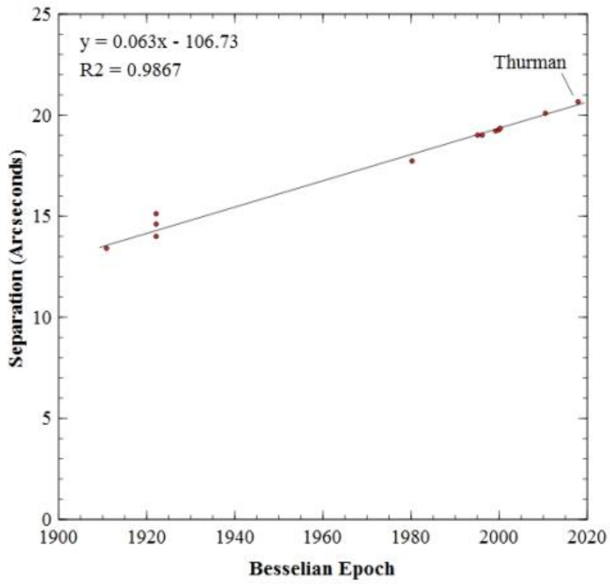

Figure 9a. WDS 07328-2332 Separation vs. Besselian Epoch.

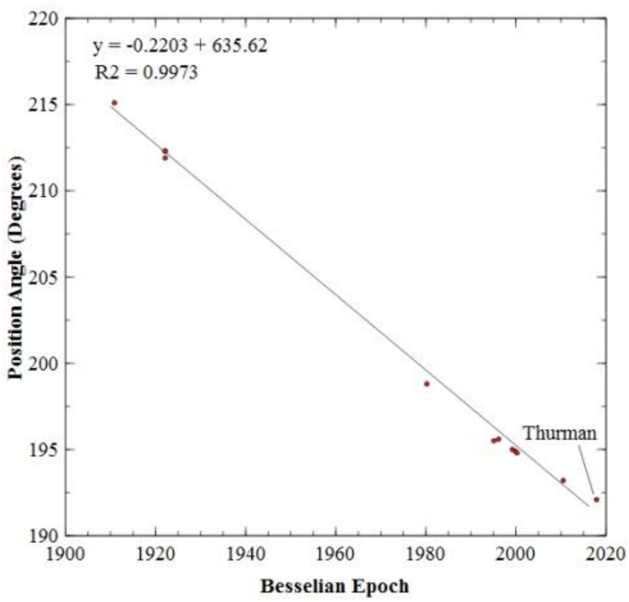

Figure 9b. WDS 07328-2332 Position Angle vs. Besselian Epoch.

Appendix 2: Motion of the Secondary Star, in Cartesian Coordinates.

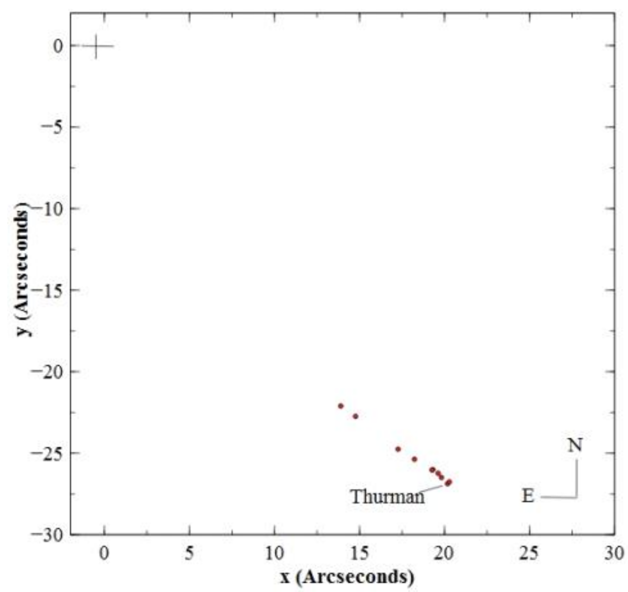

Figure 1. WDS 01588+0908 Motion of Secondary, Cartesian Coordinates.

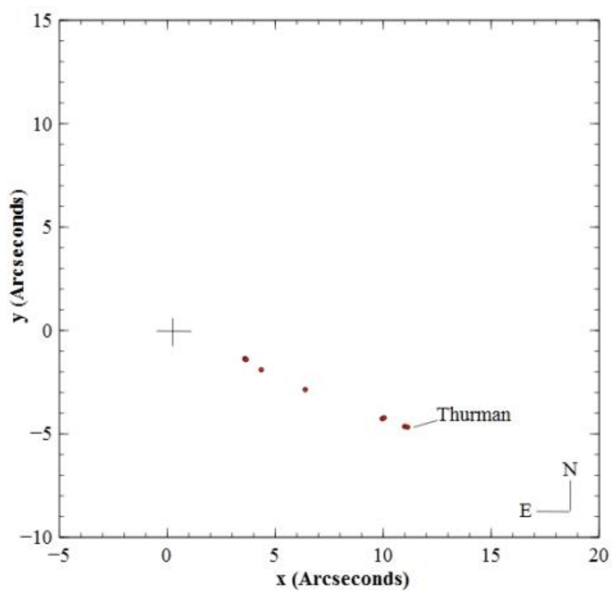

Figure 2. WDS 03002-1110 Motion of Secondary, Cartesian Coordinates.

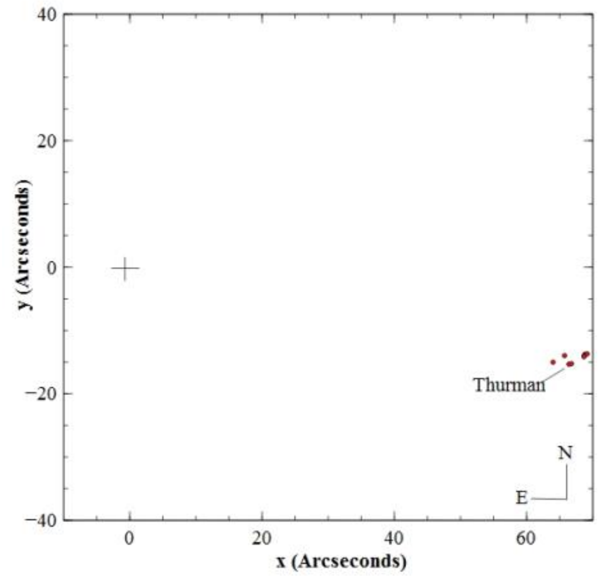

Figure 3. WDS 04528-2521 Motion of Secondary, Cartesian Coordinates.

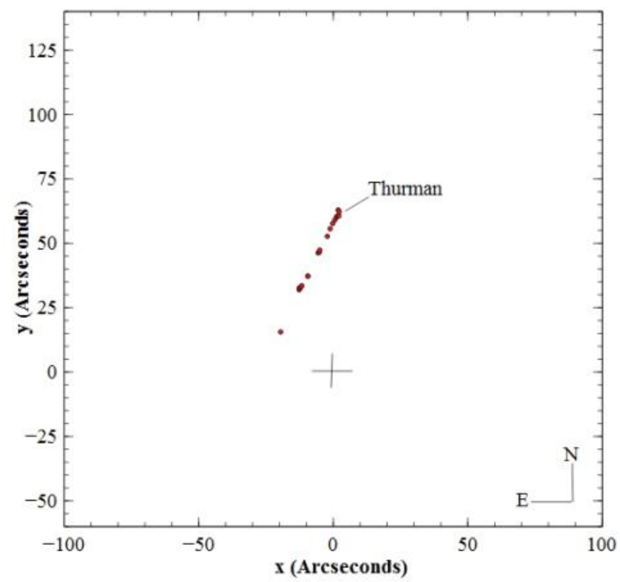

Figure 5. WDS 06171-2243 Motion of Secondary, Cartesian Coordinates.

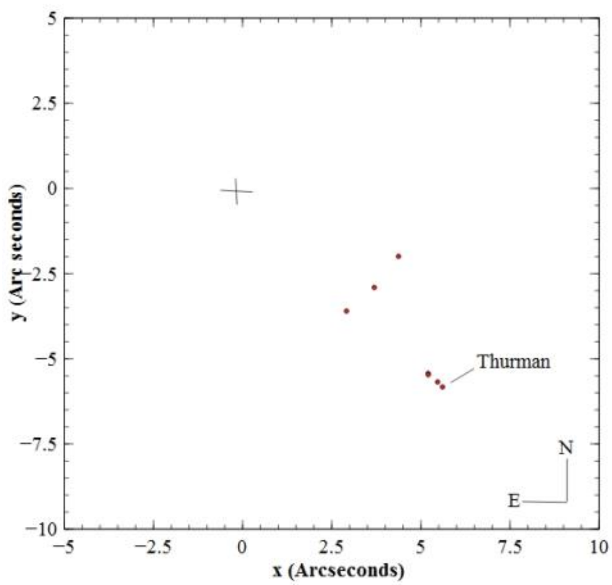

Figure 4. WDS 04530-2758 Motion of Secondary, Cartesian Coordinates.

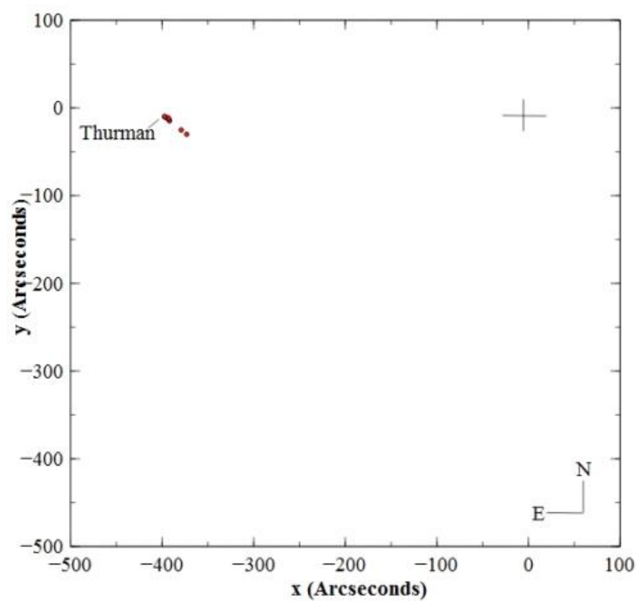

Figure 6. WDS 06377+6129 Motion of Secondary, Cartesian Coordinates.

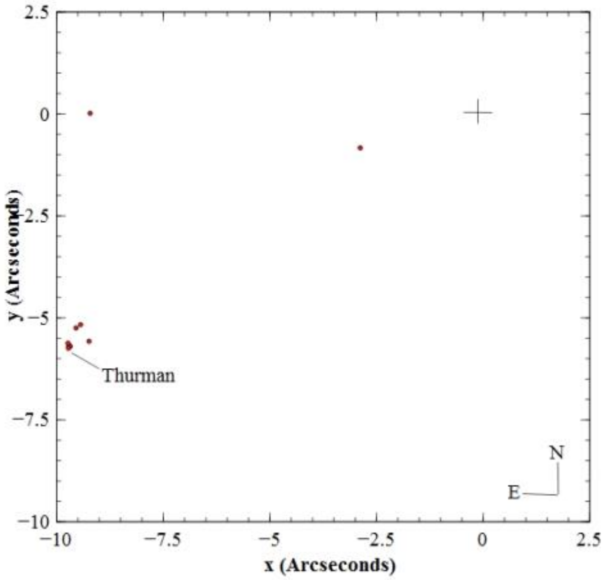

Figure 7. WDS 06389-2846 Motion of Secondary, Cartesian Coordinates.

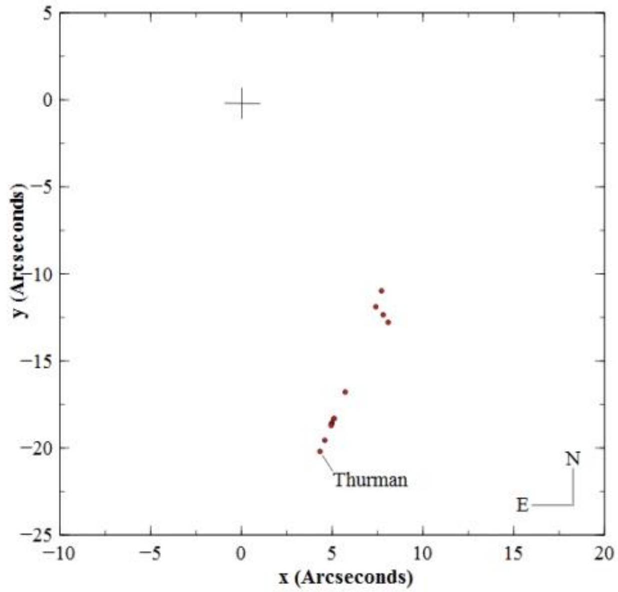

Figure 9. WDS 07328-2332 Motion of Secondary, Cartesian Coordinates.

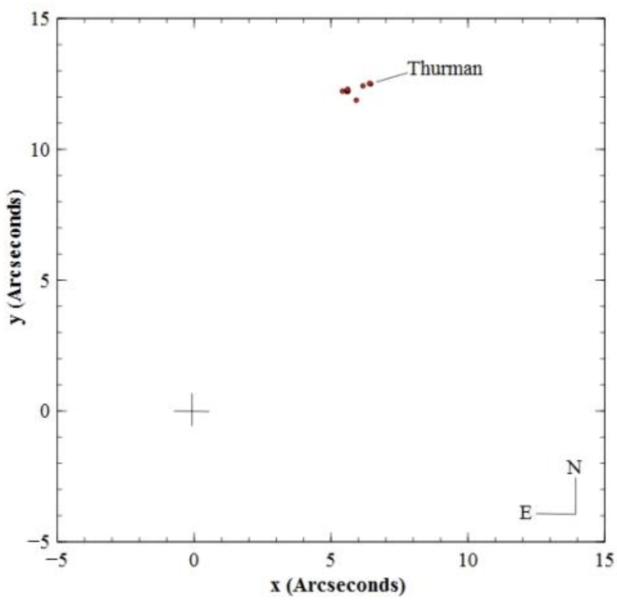

Figure 8. WDS 07317-2356 Motion of Secondary, Cartesian Coordinates.